PREVENTING DYNAMIC ROLLOVER IN BROWNOUT

Alexander Gatter, alexander.gatter@dlr.de, German Aerospace Center (DLR)

Abstract
The Institute of Flight Systems at the DLR (German Aerospace Center) site in Braunschweig, Germany is trying to find ways to improve the safety of helicopter operations. One very dangerous type of operation that is the landing of a helicopter. Loss of situational awareness can lead to unwanted contact with objects or a dynamic rollover when touching the ground. This paper presents research with optical navigation methods that has been conducted towards minimizing the danger of a dynamic rollover in bad visual conditions. Optical navigation is a method that is often used for navigating small unmanned aircraft. However, the so far conducted research in that field usually focuses on undegraded visual environment. Most of the optical navigation methods are designed to work with images that can fully be evaluated. In this paper, a set of existing optical navigation methods is tested towards the ability to work in degraded visual environment. Further, a self-developed method is presented that has been designed to be abe to work in scenarios where most parts of an image cannot be evaluated. The methods are tested on recorded flight test data. These flight test data are modified with a set of masks that simulate a visibility impairment. The conducted tests show that existing optical navigation methods do struggle when the complete image area cannot be evaluated. The evaluation of the self-developed method shows that it is not affected by impaired sight. However, its performance in situations with non-restricted sight shows to be behind the performance of some of the existing methods.

1. INTRODUCTION

This paper addresses the problem of excessive lateral speed during helicopter landing approaches. Excessive lateral speed can lead to a dynamic rollover when the landing skid gets stuck on obstacles or on rough surfaces. If the lateral movement of the helicopter is not counteracted in time, the movement leads to an angular movement around the contact point of the surface and the landing skid, causing a dynamic rollover. Pilot surveys resulted a maximal tolerable lateral speed of 0.5 m/s to 1.5 m/s in order to avoid dynamic rollovers, depending on the roughness of the surface.
Since dynamic rollovers are closely connected to the lateral speed of the helicopter, a situational awareness of the lateral speed of the helicopter is key to prevent dynamic rollovers. The speed of the helicopter can be estimated in different ways.

Copyright Statement
The authors confirm that they, and/or their company or organization, hold copyright on all of the original material included in this paper. The authors also confirm that they have obtained permission, from the copyright holder of any third party material included in this paper, to publish it as part of their paper. The authors confirm that they give permission, or have obtained permission from the copyright holder of this paper, for the publication and distribution of this paper as part of the ERF proceedings or as individual offprints from the proceedings and for inclusion in a freely accessible web-based repository.

- The helicopter pilot can estimate the speed by observing the movement of the surface in relation to the helicopter.
- Inertial Navigation Systems (INS) can provide an estimation of the speed of the helicopter by integrating the accelerations that are measured with Inertial Measurement Units (IMU) .
- Position estimations from Global Navigation Satellite System (GNSS) data can be derived in order to estimate the speed of the helicopter.
- The two aforementioned approaches can be combined into an Integrated Navigation System (INS/GNSS).
- Active optical sensors like radio detection and ranging (radar) systems or light detection and ranging (lidar) systems can measure the helicopter speed by time-of-flight measuring or via Doppler shift of their signals.
- Passive optical sensors like conventional television cameras (TV) or infrared (IR) cameras.

Visually observing the vicinity of the helicopter is the most widespread approach to detect an imminent dynamic rollover. However, pilots are not always able to correctly estimate the lateral speed of the helicopter. Especially student pilots are prone to cause dynamic rollovers (e.g. see [1,2,3]). Another phenomenon, that impedes the pilots ability to detect

This work is licensed under the Creative Commons Attribution International License (CC BY). Copyright © 2019 by author(s).

an imminent dynamic rollover is brownout, which will be focused in the presented paper. Brownout can occur when a pilot is landing on a non-paved sandy surface. The downwash of the rotor can then stir up dust particles, drenching the helicopter in a sand cloud and therefore rendering the pilot nearly blind. An INS estimates the movement speed of the helicopter by integrating over the measured accelerations. Errors in the measured accelerations cannot be corrected. Therefore, the speed estimation deteriorates over time, rendering an INS unfeasible for longer flights. INS/GNSS data are able to measure the movement speed of the helicopter with sufficient accuracy. But if GNSS data are not available (e.g. when flying in canyons or due to jamming), these systems also cannot be used for estimating the movement speed of the helicopter. Active optical sensors are also able to detect the lateral movement speed of the helicopter with sufficient accuracy. Both lidar and radar are able to penetrate dust clouds[4]. However, small radar or lidar systems provide little use besides detecting the movement speed (in general, sensors which can fulfill several purposes are favored in aircraft) while larger systems are expensive and power consuming. Another downside of these systems is that helicopters are often not equipped with these. Attaching sensors can be a time and money consuming effort. Passive optical sensors can be used to sufficiently detect excessive lateral movement speed in scenarios without Degraded Visual Environment (DVE)[5,6]. Another benefit of passive optical sensors is that they are cheap, consume little power and many helicopters are already equipped with them.

2. OPTICAL NAVIGATION IN BROWNOUT

Unlike active optical sensors, passive optical sensors are not able to penetrate dust clouds[4]. However, there is a phenomenon in helicopter brownout landings that enables optical navigation up to a certain point: when a helicopter is flying closely above the surface in a brownout cloud, the so-called donut effect is established. The donut effect is caused by the downwash of the helicopter that circulates away from the helicopter cell. With this, a region below the helicopter is mostly kept free from stirred up dust and therefore can be used for optical navigation applications. Figure 1 shows the sketch of a donut effect.

During the war in Afghanistan, the CH-53 helicopters which were operated by the German forces utilized the donut effect by using a member of the crew as an observer of the helicopters relative movement to the ground. To get a clear viewing of

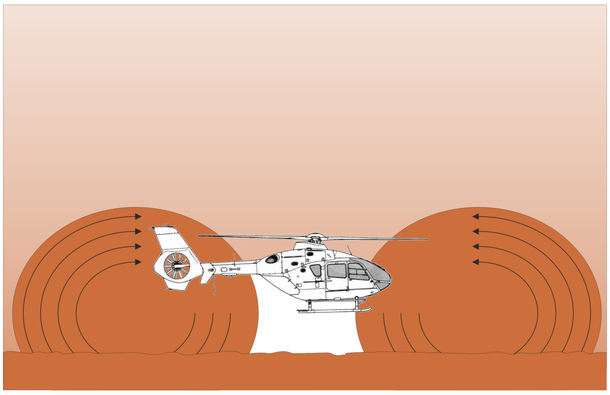

Figure 1: Sketch of a donut effect.

the surface, the crew member hat to view out of the helicopter through the opened tailgate. This process was time-consuming and led to the German helicopters having to stay for a long time in the brownout clouds, increasing the danger of hostile fire and getting damaged by the dust particles. Substituting the process of a crew member having to look out of the tailgate by utilizing a passive camera and performing an automated evaluation of the lateral movement speed of the helicopter can speed up the landing process significantly (tests on optical navigation methods which are presented in this paper show that a valid movement estimation can be given in less than five seconds).

Since most cameras are mounted below the helicopter in a forward-looking or slightly downward-tilted way, some areas close to the lower border of the camera images are not affected by the brownout.

Optical navigation methods are usually designed to work with images that can be fully evaluated. The most common approaches to perform optical navigation are Visual Simultaneous Localization And Mapping (VSLAM), Visual Inertial Simultaneous Localization And Mapping (VISLAM), Visual Odometry (VO), and Visual Inertial Odometry (VIO). These methods work either directly on the images or use extracted and described image features for estimating the movement of the camera. Another approach to estimating the movement of a vehicle is to directly evaluate the optical flow of an image sequence. The above-mentioned methods try to separate the observed movement of the scenery into its rotational and translational components. The separation of the two movement components usually facilitates, that translational movement is affected by the parallax phenomenon, resulting in a reduced observable movement in distant image regions. All these approaches have in common, that they never have been tested on their applicability to brownout

This work is licensed under the Creative Commons Attribution International License (CC BY). Copyright © 2019 by author(s).

situations where you only have a restricted image area in which an evaluation is possible. With these image regions being located at the lower border of the camera image, the parallax effect cannot be utilized.
Besides the sight restriction caused by brownout, another phenomenon that can have a detrimental impact on optical navigation methods has to be regarded: the self-cast shadow of the helicopter. Flying close to the surface, the self-cast shadow can cover substantial parts of the image regions that are being kept free from disturbances by the donut effect. Optical navigation methods rely on the observed scenery being static. The self-cast shadow of the helicopter creates a movement on the surface that can lead to false movement estimations if the optical navigation methods create their movement estimation based on the shadow movement. Since unlike human perception, optical navigation methods cannot easily distinguish between shadows cast by the scenery and shadows which are cast by the helicopter, the self-cast shadow of the helicopter has to be identified in order to prevent a detrimental effect on the optical navigation method. This can be achieved by applying the algorithm which was presented in [6,7].
Since no flight tests in brownout situations could be conducted, a synthetic scene that simulates the restricted sight which is caused by the brownout is used instead. This synthetic scene is created by using the freely available software *blender*. This tool has been set up to be able to create synthetic dust clouds based on a physical dust simulation dependent on given flight state data (mostly height above ground). However, the physical model behind the dust simulation was not accessible. Because of that, the dust simulation has been parametrized to mirror the brownout behavior of freely available videos from on-board cameras of helicopters landing in brownout situations. The videos that have been used also contained video footage from the helicopters instruments during the landing approaches, showing the height above ground of the helicopter paired with the developed brownout as it is visible for the camera that is mounted on the outside of the helicopter. Also, the mount angle of the camera was known. With all this information, a realistic behavior of the dust clouds can be created. The synthetic dust clouds are used to create masks with which parts of an image can be blocked from further processing. Figure 2 shows a screenshot of a dust cloud that has been simulated with the brownout tool as well as a mask which has been created by the tool applied to a recorded image from a flight test.

(a) Screenshot of the brownout simulation tool.

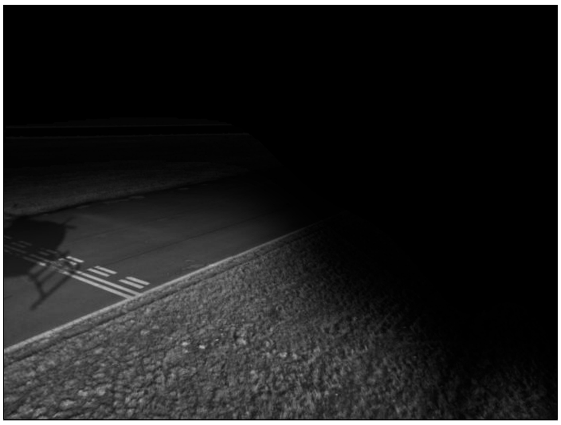

(b) Resulting mask applied to a camera image.

Figure 2: Brownout simulation.

Four sets of brownout masks have been created in order to test different levels of restricted sight. The size of the areas in the images which are not disturbed is gradually decreasing over these four sets. The unmodified brownout masks cover approximately 50 % of the camera images over the complete sequence. The other three sets increase the space covered by the masks by approximately 10 % each, ending with 80 % of the images covered for the last set of brownout masks.

With the so far identified demands, the ideal motion estimator for the set task has to be able to:

- estimate the helicopter speed sufficiently precise,
- work in DVE, and
- quickly create a speed estimation.

Several optical navigation methods have been selected to be tested regarding their ability to meet these demands. These methods are the VSLAM method ORB-SLAM [8], the VO method LIBVISO2 [9], a modified version of the tightly coupled VIO method

This work is licensed under the Creative Commons Attribution International License (CC BY). Copyright © 2019 by author(s).

from Troiani[10] and a self-developed tightly coupled method that is based on optical flow. In the next chapter, the existing methods will be introduced and the self-developed algorithm will be presented in detail.

2.1. Existing methods

Commonly available optical navigation methods (VO and VSLAM) are designed to create robust long-term movement estimations. For this, they usually need a rather long initialization phase

ORB-SLAM is a VSLAM-based approach. An implementation of this approach is freely available*. The method performs a multitude of processing steps and optimizations. The most important are

- a short term estimation of the movement of a vehicle by using two different approaches (computing a homography and computing an essential matrix) of which the most robust one is taken for further estimations,
- setting up a map of the vicinity of the vehicle that then is used to locate the vehicle in,
- a bundle adjustment step that optimizes over several of the last movement estimations, setting keyframes when a movement estimation is regarded as being reliable, and
- a loop closing step that tries to conduct global optimizations of the map when a place in the map is revisited, applying modifications to the map as well as the existing keyframes.

The (monocular) VO method from LIBVISO2† does estimate the movement of a vehicle by only computing an essential matrix. The method also does not create a map of the vicinity and therefore also performs no loop closing. Movement estimations are solely generated by keyframes which cannot be modified anymore once they are set. Short term optimizations via bundle adjustment are still performed. The monocular implementation of LIBVISO2 calculates the scaling factor of the movement estimation with a set of assumptions that only can be met with a camera that is rigidly attached to a moving car. Therefore, the code of LIBVISO2 has been altered to get the scaling factor from a sequence of 100 frames with known translational movement. This implies, that in order to use this VO approach, the method has to have some time for initializing before entering brownout.

*`https://github.com/OpenSLAM-org/openslam_orbslam`

†`http://www.cvlibs.net/software/libviso/`

The tightly coupled VIO method is implemented as an extension of the LIBVISO2 code. It is based on the method of Troiani which projects the tracked features of two to-be-compared time steps onto a two independent unit spheres and then transforms one unit sphere into the coordinate system of the other unit sphere (taking angular movement data from an IMU) and then expresses the epipolar geometry in relation of two angles and a scale factor. The modified approach expresses the epipolar geometry in relation of the x-, y-, and z-translation. The transformation of the projected features has been implemented accordingly in the LIBVISO2 code. The calculation of the epipolar geometry has been kept unchanged.

2.2. Self-developed method

The self-developed method has been designed to meet the requirements that have been postulated in chapter 2. It uses two different feature extractors and feature trackers:

- the feature extractor from Shi and Tomasi[11], which is extended to be scale invariant with the feature tracking approach from Lukas and Kanade[12] and
- the ORB feature extractor and descriptor[13].

The method from Lukas and Kanade works fast and robust and has proven to produce good results in airborne optical navigation (see e.g.[14]). ORB has been selected because compared to more complex methods like SIFT and SURF its matching performance shows results of similar quality while being significantly less time-consuming[15].
Also, the two methods inherit different working principles. The feature extractor and tracker from Shi and Tomasi is designed to perform a local search for reoccurring contrast patterns in subsequent images evaluating the local optical flow. ORB creates feature vectors which describe an image region and then globally compares feature vectors of sets of image regions in subsequent images. The decision to use two feature extractors has been made because of a set of arguments:

- Empirical tests have shown, that both feature extractors tend to select different image regions, therefore increasing the chance of extracting a sufficiently large set of features for conducting the movement estimation.
- Introducing a redundant method increases the robustness of the created method.
- With the two methods having little processing time, a real time operability can be sustained.

This work is licensed under the Creative Commons Attribution International License (CC BY). Copyright © 2019 by author(s).

Since brownout should only occur during the final stage of a landing approach, the surface is expected to be plane. Therefore, the self developed method is designed, using a plane earth assumption. In addition to this assumption, the algorithm is designed to use a set of sensor data that is commonly available:

- The orientation of the helicopter and
- the height above ground of the helicopter.

The self developed algorithm is inspired by the method presented in[5], using the mathematical description of the optical flow in a sequence which goes back to Higgins and Prazdny[16]. This description uses a pinhole camera model with an orthographic projection. The method tries to determine the optical flow that is generated by the rotational movement of the helicopter by using IMU data. By having the rotational component of the optical flow, the translational component can easily be obtained. In the following, the process to get the translational component of the optical flow and with it the absolute movement of the helicopter is explained.
The movement $(u,v)^T$ of projected points $(x,y)^T$ in image space in x- and y-direction is calculated by the translational (T_{im}) and rotational (Ω_{im}) camera movement in image space of the cameras translational (T) and rotational (Ω) movement in camera space.

$$(1)\quad \begin{pmatrix} u \\ v \end{pmatrix} = T_{im} + \Omega_{im}$$

with

$$(2)\quad T_{im} = \begin{pmatrix} -f & 0 & x \\ 0 & -f & y \end{pmatrix} \begin{pmatrix} T_x \\ T_y \\ T_z \end{pmatrix}$$

and

$$(3)\quad \Omega_{im} = \frac{1}{f} \begin{pmatrix} xy & -f^2 - x^2 & fy \\ f^2 + y^2 & -xy & -fx \end{pmatrix} \begin{pmatrix} \Omega_x \\ \Omega_y \\ \Omega_z \end{pmatrix}$$

where f is the focal length of the used camera.
Formula (1) is then solved for T_x and T_y resulting in

$$(4)\quad \begin{pmatrix} T_x \\ T_y \end{pmatrix} = \frac{1}{f} \begin{pmatrix} T_z x - uz \\ T_z x - vz \end{pmatrix} + \frac{z}{f^2} \begin{pmatrix} xy\Omega_x - (f^2+y^2)\Omega_y + fx\Omega_z \\ (f^2+x^2)\Omega_x - xy\Omega_y - fy\Omega_z \end{pmatrix}.$$

Flight state data (FSD) usually is given in a coordinate system that is aligned with the helicopter coordinate system. Cameras often are not fully aligned with the helicopter coordinate system but are attached to the helicopter with a downward tilt angle θ_c. In order to simulate the optical flow that is caused by the helicopter movement, the coordinate system of the camera has to be transformed into a north east down (NED) coordinate system. This is achieved by aligning the optical axis of the camera image with the x-axis of the helicopter coordinate system corrected by the negative helicopter pitch angle θ_h. For this, the horizontal aperture angle $\omega_{i,vert}$ of the camera is calculated with

$$(5)\quad \omega_{i,vert} = 2\tan^{-1}\left(\frac{y_{i,max} - y_{i,min}}{2f}\right).$$

This angle is then used to align the vertical part of the optical axis o_y with the helicopter x-axis with

$$(6)\quad o_y = \frac{y_{i,max} - y_{i,min}}{2} - \frac{(y_{i,max} - y_{i,min})\theta_c}{\omega_{i,vert}} + \frac{(y_{i,max} - y_{i,min})\theta_h}{\omega_{i,vert}}$$

and then adjust all image points (x_i, y_i) according to o_y. Cameras may also be attached with a horizontal angle that differs from the helicopter coordinate system. Since cameras usually are not mounted with an horizontal angle, the correction of non-aligning horizontal angles are not treated in this paper.
One variable of (4) is yet to be determined: The translation T_{z_c} in the movement direction. This movement is estimated by measuring the change in distance of the tracked image features. The distance of a feature is estimated by using a plane earth assumption, the known attitude of the camera and the intrinsic parameters of the camera.
First, the angles of all n features in camera space are extracted with

$$(7)\quad \alpha_{x_i} = tan^{-1}\left(\frac{o_{x_i}}{f_x}\right) \quad \forall i \in [1;n]$$

and

$$(8)\quad \alpha_{y_i} = tan^{-1}\left(\frac{o_{y_i}}{f_y}\right) \quad \forall i \in [1;n].$$

For this calculation, the non-modified optical axis o is used which is not corrected for the vertical mount angle of the camera. Next, a normalized direction vector $P = (0,0,1)^T$ is created for each feature. These direction vector points P_{c^i} in the camera coordinate system are then rotated with their respective internal angles $\alpha_{x,y}$ and the mounting angle of

This work is licensed under the Creative Commons Attribution International License (CC BY). Copyright © 2019 by author(s).

the camera in relation to the helicopter to transform them into helicopter coordinate system points P_{h^i}. A line can be expressed with

(9) $\quad P_2 = P_0 + dP_1$ with $d > 0$

where P_0 is the origin point of the line and P_1 is one of the points P_{h^i} in the helicopter coordinate system that is scaled with a factor d. By parametrizing a plane in hessian form

(10) $\quad E : P_3 \cdot P_2 + P_4 = 0,$

with P_{2-4} being the parameters that span the plane E, putting (9) into (10), and solving for d gives

(11) $$d = \frac{-\left(P_3 \cdot P_0 + P_4\right)}{P_3 \cdot P_1}.$$

Here, d is representing the depth of the scene z. The to be subtended plane is set to $(0, 0, 0)^T$. With this, P_4 can be taken out of the equation. The origin and the position of the helicopter is set to $P_0 = (0, 0, h)^T$ with h being the height above ground of the helicopter. The normalized form of the plane is set to

(12) $$P_3 = \begin{pmatrix} 1 \\ 0 \\ 0 \end{pmatrix} \times \begin{pmatrix} 0 \\ 1 \\ 0 \end{pmatrix} = \begin{pmatrix} 0 \\ 0 \\ 1 \end{pmatrix}.$$

With P_3 only containing values in its z-component, the this (11) can be simplified to

(13) $$z = \frac{h}{z_{h^i}} \quad \forall i \in [1; n]$$

substituting d with z. Over the theorem of Pythagoras the distance z' on ground between feature and helicopter can be obtained with

(14) $$z' = z \cos \sin^{-1}\left(\frac{h}{z}\right).$$

The final directional movement estimation T_{z_c} is then computed by averaging all n $\Delta z'$ for one time step.
With all elements of (4) available, the lateral speed estimation for the camera V_{y_c} for two time steps is finally computed with

(15) $$V_{y_c} = \frac{T_{y_c}}{\Delta t}.$$

Transforming the lateral camera movement speed into the helicopter coordinate system yields V_{y_h}.

In order to reduce noise in the movement estimation which is caused by discretization effects of the camera pixels, the movement estimation is not computed by each two consecutive time steps. The movement estimator instead tries to track features over a longer period of time and computes a movement estimation between the time of the extraction of the feature and the current time. For this estimation, a short-term constant movement speed of the helicopter is assumed. In order to minimize discretization effects, a minimal difference of 5 time steps Δt_5 is set for the evaluation of a tracked feature. The maximal time between two comparisons is set to 0.5 s. If a feature is tracked for a longer period, the feature is compared to the position it had 0.5 s before. Therefore, the formula for creating a movement estimation for one feature is given by

(16) $$V_{y_h} = \begin{cases} \frac{T_{y_h}}{\Delta t_d}, & \text{for } t_{max} \geq \Delta t_5 \\ \varnothing, & \text{for } t_{max} < \Delta t_5 \end{cases}$$

with

(17) $$\Delta t_d = t_0 - \min(t_{max}, 0.5\, s).$$

Having a look at all $n = k + l$ features, we get two lists

(18) $$V_{ORB} = \left[V_{y_{0,ORB}}, V_{y_{1,ORB}}, ..., V_{y_{k,ORB}}\right]$$

(19) $$V_{LK} = \left[V_{y_{0,LK}}, V_{y_{1,LK}}, ..., V_{y_{l,LK}}\right]$$

of movement estimations.
In order to compensate outliers, the median values $\tilde{V}_{LK}$ and $\bar{V}_{ORB}$ are computed and the 10 % of the estimations that have the strongest deviation from this mean value are removed. After that, $\bar{V}_{LK}$ and $\bar{V}_{ORB}$ are computed again with the reduced set of estimations.
In order to warrant the robustness of the individual movement estimators, the minimal amount of detected features has been set to 20. If at least 20 successfully tracked features are left after the outlier removal, the set of features can be used for the final lateral movement speed estimation V with

(20)
$$V = \begin{cases} \frac{\bar{V}_{LK} + \bar{V}_{ORB}}{2}, & \text{for } |V_{LK}| \geq 20,\ |V_{ORB}| \geq 20 \\ \bar{V}_{LK}, & \text{for } |V_{LK}| \geq 20,\ |V_{ORB}| < 20 \\ \bar{V}_{ORB}, & \text{for } |V_{LK}| < 20,\ |V_{ORB}| \geq 20 \\ \varnothing, & \text{else.} \end{cases}$$

3. FLIGHT TESTS

The selected methods are applied to a flight test that has been recorded by the Active Control Technology/ Flying Helicopter Simulator (ACT/FHS), a

This work is licensed under the Creative Commons Attribution International License (CC BY). Copyright © 2019 by author(s).

highly modified EC 135 that is operated by the DLR. The ACT/FHS has a rotor diameter of 10.2 m and a maximal takeoff weight of 2910 kg. The on-board camera that was used to record the image sequence of the recorded flight test is a AVT Guppy-PRO with a $68^\circ \times 49^\circ$ field of view, a 17 Hz frame rate, and a resolution of 694×519 pixels. A photograph of the ACT/FHS is displayed in Fig. 3. The flight test was recorded at a meadow next to the runway of the airport of Braunschweig, Germany. The evaluated sequence consists of 200 images and has a duration of 11.72 s and has been selected because it contains a lateral movement of the helicopter close to the ground as well as the self-cast shadow of the helicopter. During the sequence, the ACT/FHS performs a mostly lateral flight while also turning around its z-axis. Its lateral speed stays at approximately 2.3 m/s during the first 80 % of the sequence and then slows down to 1.4 m/s over the last 20 % of the sequence. The height above ground stays in the range from 3.1 m to 4.5 m. The self-cast shadow of the helicopter is visible in all 200 images. A set of images which are taken from this sequence is displayed in Figure 4.

The self-cast shadow regions have been correctly excluded from further processing in 98 % of all frames using the shadow detector described in[6,7].

Next, the brownout masks are applied to the images. Finally the movement estimators are tested on the original unmodified image set as well as on the image sets that have been modified with the brownout masks. The results that have been achieved are presented in the following. These evaluations pictured for the different movement estimators show the deviation of the estimated movement speed, given in its lateral component for the current heading angle of the helicopter from recorded lateral movement reference data. The reference data is retrieved by taking position data which has been recorded by differential global positioning system (DGPS) signals combined with data from a Honeywell H-764 ACE INS. The reference data have been recorded with a frequency of 31 Hz. The plots also contain the identified limits of lateral movement speed which have not to be breached in order to ensure safe landing on rough or normal surfaces. With keeping the deviations of the estimated movement speed below these thresholds and assuming an indicated movement speed of 0 m/s, the respective movement estimator is able to be used to predict the threat of a dynamic rollover.

Figure 3: Photograph of the ACT/FHS.

3.1. VO-based Movement Estimator

First the application of LIBVISO2 to the image sets is evaluated. These results are depicted in Figure 6. Here, a movement estimation is created for each recorded camera image. As can be seen, even in the non-disturbed image set, the movement deviation has a significant amount of spikes that deviate for more than 1 m/s from the reference movement speed. The estimated movement speed even gets worse, once parts of the images are covered by dust. With this, LIBVISO cannot be used for estimating the lateral movement speed of a helicopter in any circumstance and on any surface. Investigations for the reasons for these bad results did lead to the conclusion, that the fundamental matrix calculation has problems with separating the feature movement in image space into its lateral and rotational components because of the flatness of the surface of the scenery. Tests with recorded flights that took place in non-flat scenery did yield significantly better results for non-disturbed image sets. In these non-disturbed scenarios, a safe landing on normal and rough surface can be guaranteed by LIBVISO2. However, introducing DVE still leads

Figure 4: Pictures from different time steps of the evaluated flight test.

This work is licensed under the Creative Commons Attribution International License (CC BY). Copyright © 2019 by author(s).

to a significant degradation of the reliability of the method. Therefore, the method cannot be used for detecting the danger of a dynamic rollover landing.

3.2. VIO-based Movement Estimator

The VIO-based movement estimator improves the robustness of the LIBVISO2 approach by aiding the separation of the movement components easier with providing the rotational movement data. In this approach, only the movement estimation that has been created by the keyframes is used for estimating the movement speed of the helicopter. Keyframes are set dependent on the reliability of a movement estimation and also dependent on the changing of the scene. The faster a scene changes (i.e. higher translational or lateral movement speed as well as high rotational speed), the more regularly they are set. Therefore, it can be guaranteed that between to keyframes there are no excessive changes in the movement behavior of the helicopter (In the tests with the unmodified LIBVISO2 method, using keyframes still would not have yielded better results). The results of the application of this method to the flight test are depicted in Figure 7. As can be seen, the method creates a significantly improved movement estimation over the result from LIBVISO2 in the unmodified image set. Only one keyframe has a deviation 0.537 m/s and therefore breaches the postulated limit of 0.5 m/s for safe landing on arbitrary surface. As this limit is only breached for one single time step, even a landing on arbitrary surface can be regarded as still being sustainable. Introducing DVE however instantly renders the method to be not usable anymore. Even for a slightly degraded sight, the deviation of the movement estimation climbs up to 2 m/s. Therefore, the use of this method in brownout situation is not advisable.

3.3. SLAM-based Movement Estimator

The evaluation of the application of ORB-SLAM to the test sequence is shown in 8. Here, again only keyframes are used for estimating the lateral movement speed. As can be seen, the deviation of the movement estimation from the reference data is even smaller than for the VIO-based method. The maximal deviation is 0.39 m/s, so the safety margin for landing on arbitrary surface is 0.11 m/s. Looking at the evaluations of the image sets with degraded sight shows, that the performance of ORB-SLAM is decreasing as the simulated brownout regions are consuming larger parts of the images. With the second set of brownout masks, the deviation breaches the 0.5 m/s limit in one time step, reaching a deviation of 0.52 m/s. In the third set of brownout masks, the 0.5 m/s limit is breached at 8.3 s of and stays above that limit for the rest of the sequence. In the last set of brownout masks, the deviation of the speed estimation is further increasing, now even violating the 1 m/s limit in seven frames.
A second phenomenon can be observed in the evaluated flight test scene: the initialization of the map takes some time. In each set of the images, the initialization phase takes about 4 s. Since the time of staying in brownout should be kept minimal, this is at least a hindrance. However, overall it can be stated that ORB-SLAM is able to create reliable movement estimations in scenarios with little or moderately degraded sight and enough time for initialization.

3.4. Self Developed Movement Estimator

The evaluation of the application of the self developed method to the test scene is shown in 9. It was designed to give a fast estimation of the movement speed and to work independent from degraded sight. Indeed it can be seen, that it does provide a movement estimation nearly instantly and that its performance, as the only evaluated method, is not decreasing with an increase of the brownout regions. However, its maximal deviation is notably higher than the movement estimation that is generated by ORB SLAM. In all shown graphs, the deviation is breaching the postulated limit of 0.5 m/s, therefore rendering the method not applicable to landings on rough surfaces. However, as the only tested method, the maximal deviation stays below 1 m/s all the times, although it is close to 1 m/s. To further investigate that the error is not just below 1 m/s due to the shortness of the sequence, the self developed movement estimator has been applied to a longer sequence (adding about 20 s to the reference test sequence). The results of this test are displayed in figure 5. In this longer sequence, the error also does not exceed the 1 m/s limit. The evaluation of the test sequence indicates that a safe landing in brownout scenarios can be conducted if an a priori knowledge of the flatness of the landing site is available.

4. CONCLUSIONS

In the presented paper, several different methods to estimate the movement speed of a helicopter during landing approaches with and without DVE were tested. The tests resulted in no method being able to meet all the postulated demands for guaranteeing a safe landing without the danger of dynamic

This work is licensed under the Creative Commons Attribution International License (CC BY). Copyright © 2019 by author(s).

rollover. However, two methods have shown good results if the postulated demands are slightly softened. A combination of these two methods has the potential to decrease the required amount of softening up the postulated demands. This means combining the self-developed method with ORB-SLAM in a way, that the self-developed algorithm delivers movement estimations during flight phases with heavily reduced sight while ORB-SLAM is initializing and then switching to ORB-SLAM once it has finished its initialization phase and the sight degradation is lessened (which usually happens when getting closer to the ground).
Summarizing, it can be stated that optical navigation has the potential to be used to detect the threat of dynamic rollovers, being advisable as redundant movement estimators for flight students and to decrease the time that helicopter pilots have to stay in brownout.

REFERENCES

[1] Air Accident Investigation Unit (Belgium), "Safety investigation report, ref. aaiu-2013-01-ebhn." [Online]. Available: https://mobilit.belgium.be/sites/default/files/downloads/13-4.pdf

[2] Civil Aviation Department The Government of the Hong Kong Special Administrative Region, "Report on the accident to robinson r22 beta ii helicopter registration b-hjn operated by the hong kong aviation club limited at shek kong airfield, yuen long on 6 october 2013." [Online]. Available: https://mobilit.belgium.be/sites/default/files/downloads/13-4.pdf

[3] National Transportation Safety Board, "Aviation accident final report, accident number era1ca187." [Online]. Available: https://app.ntsb.gov/pdfgenerator/ReportGeneratorFile.ashx?EventID=20170522X83513&AKey=1&RType=Final&IType=CA

[4] No Author, *Final Report of NIAG167 on Helicopter Operations at low Altitude Degraded Visual Environment*, http://www.cso.nato.int/ACTIVITY_META.asp?ACT=1930, NATO Science and Technology Organization, 2013.

[5] A. Gatter, H.-U. Doehler, T. Lueken, and R. Stadelhofer, "Allflight: blob-based approach to detect dangerous drift velocities during helicopter landing approaches," *CEAS Aeronautical Journal*, vol. 6, no. 1, pp. 149–159, Mar 2015.

[6] A. Gatter, "Edge-based approach to estimate the drift of a helicopter during flight," *CEAS Aeronautical Journal*, vol. 8, no. 4, pp. 705–718, Dec 2017.

[7] A. Gatter and F. Andert, "On precisely determining self-cast shadow regions in aerial camera images," in *The 2018 International Conference on Unmanned Aircraft Systems*, Dallas, TX, Jun. 2018.

[8] R. Mur-Artal, J. M. M. Montiel, and J. D. Tardos, "Orb-slam: A versatile and accurate monocular slam system," *IEEE Transactions on Robotics*, vol. 31, no. 5, pp. 1147–1163, Oct 2015.

[9] A. Geiger, J. Ziegler, and C. Stiller, "Stereoscan: Dense 3d reconstruction in real-time," in *Intelligent Vehicles Symposium (IV)*, 2011.

[10] C. Troiani, A. Martinelli, C. Laugier, and D. Scaramuzza, "2-point-based outlier rejection for camera-imu systems with applications to micro aerial vehicles," *2014 IEEE International Conference on Robotics and Automation (ICRA)*, pp. 5530–5536, 2014.

[11] J. Shi and C. Tomasi, "Good features to track," in *9th IEEE Conference on Computer Vision and Pattern Recognition*, 1994, pp. 593–600.

[12] J.-Y. Bouguet, "Pyramidal implementation of the lucas kanade feature tracker," *Intel Corporation, Microprocessor Research Labs*, 2000.

[13] E. Rublee, V. Rabaud, K. Konolige, and G. Bradski, "ORB: an efficient alternative to SIFT or SURF," *Computer Vision (ICCV), 2011 IEEE International Conference on*, pp. 2564–2571, 2011.

[14] F. Andert, "Bildbasierte Umgebungserkennung für autonomes Fliegen," Ph.D. dissertation, Technische Universität Carolo-Wilhelmina zu Braunschweig, 2011.

[15] E. Karami, S. Prasad, and M. S. Shehata, "Image matching using sift, surf, brief and orb: Performance comparison for distorted images," *CoRR*, vol. abs/1710.02726, 2017.

[16] H. Longuet-Higgins and K. Prazdny, "The Interpretation of a Moving Retinal Image," *Proceedings of the Royal Society of London. Series B, Biological Sciences Vol.208, No. 1173*, pp. 385–397, 1980.

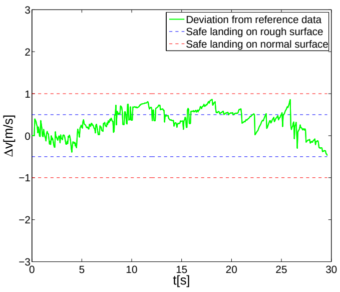

Figure 5: Movement speed estimation: Optical-flow-based approach (unmodified image set, longer sequence) in extension to Figure 9.

This work is licensed under the Creative Commons Attribution International License (CC BY). Copyright © 2019 by author(s).

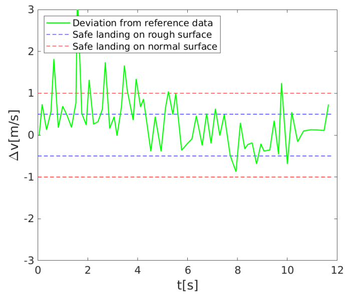

(a) Unmodified image set.

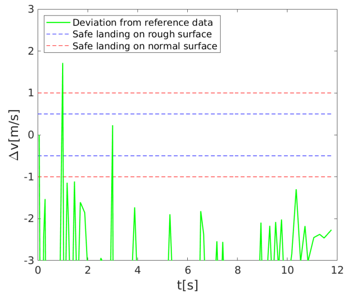

(b) Brownout masks set 1.

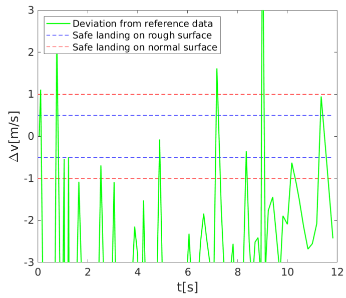

(c) Brownout masks set 2.

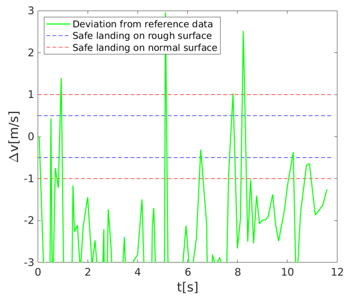

(d) Brownout masks set 3.

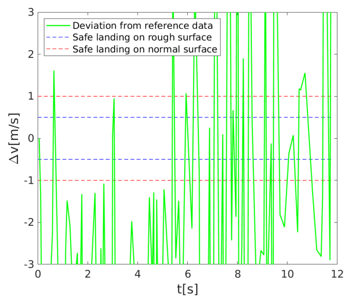

(e) Brownout masks set 4.

Figure 6: Movement speed estimation: VO-based approach.

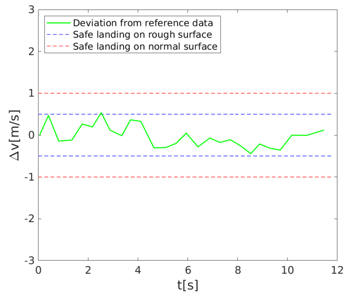

(a) Unmodified image set.

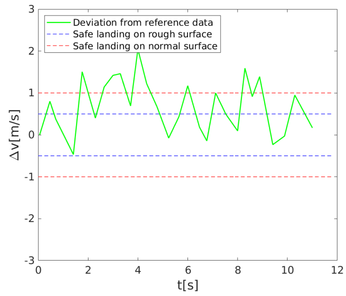

(b) Brownout masks set 1.

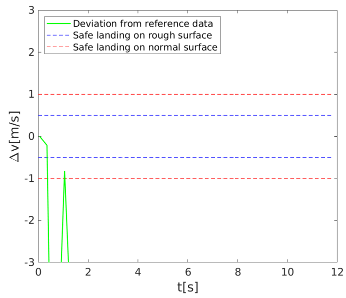

(c) Brownout masks set 2.

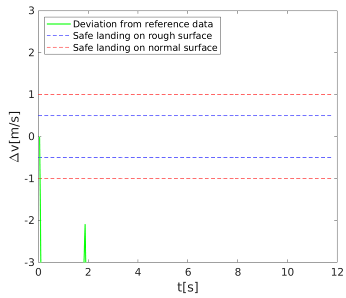

(d) Brownout masks set 3.

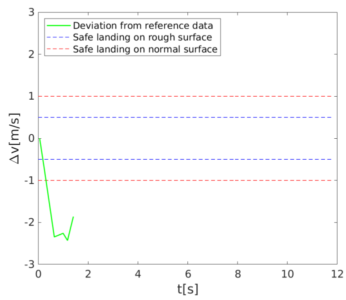

(e) Brownout masks set 4.

Figure 7: Movement speed estimation: VIO-based approach.

This work is licensed under the Creative Commons Attribution International License (CC BY). Copyright © 2019 by author(s).

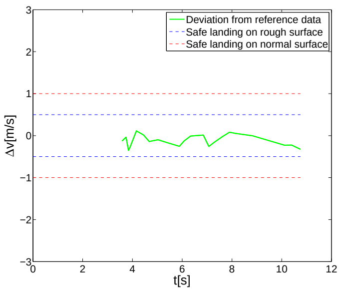

(a) Unmodified image set.

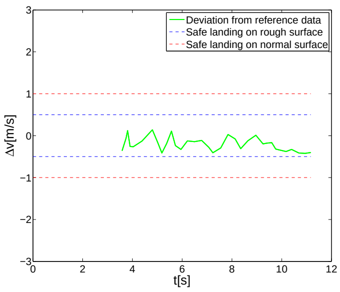

(b) Brownout masks set 1.

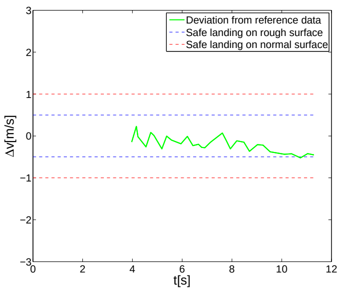

(c) Brownout masks set 2.

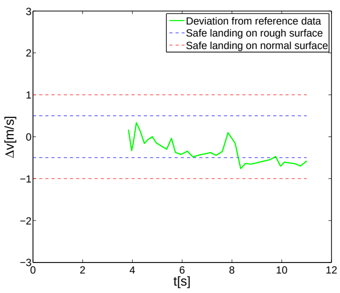

(d) Brownout masks set 3.

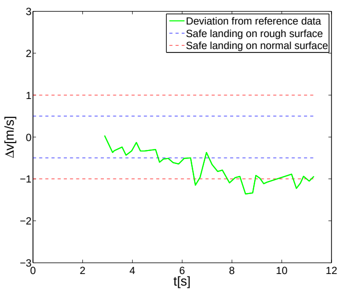

(e) Brownout masks set 4.

Figure 8: Movement speed estimation: ORB-SLAM.

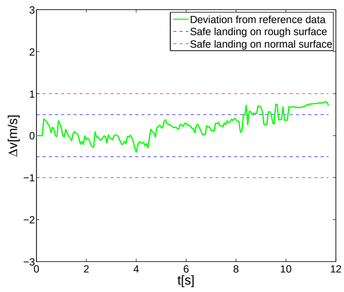

(a) Unmodified image set.

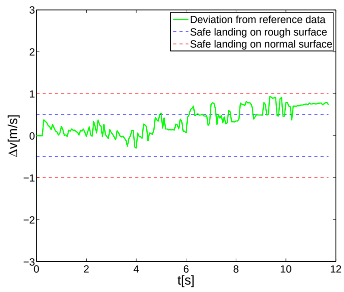

(b) Brownout masks set 1.

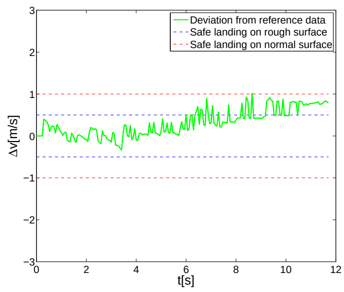

(c) Brownout masks set 2.

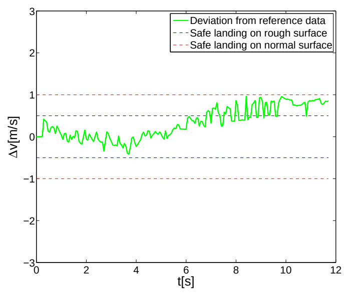

(d) Brownout masks set 3.

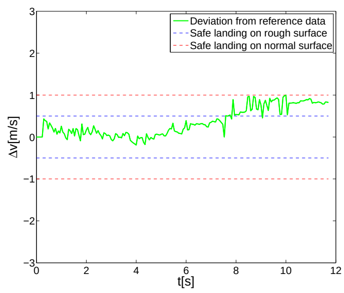

(e) Brownout masks set 4.

Figure 9: Movement speed estimation: Optical-flow-based approach.

This work is licensed under the Creative Commons Attribution International License (CC BY). Copyright © 2019 by author(s).